

# New Universality Classes in “Percolative” Dynamics

M. Ortuño,<sup>1</sup> J. Ruiz,<sup>1</sup> and J. M. F. Gunn<sup>2</sup>

*Received March 18, 1991*

---

We study a site analogue of directed percolation. Random trajectories are generated and their critical behavior is studied. The critical behavior corresponds to that of simple percolation in some of the parameter space, but elsewhere the exponents reveal new universality classes. As a byproduct, we use the model to make an improved estimate of the percolation hull exponents and to calculate the site percolation probability for the square lattice.

---

**KEY WORDS:** Percolation; external perimeter; universality; critical exponents; threshold.

## 1. INTRODUCTION

Percolation problems constitute the simplest class of systems with “phase transitions.”<sup>(1,2)</sup> The most basic types of percolation are site and bond percolation, and the latter has a directed version, where the bond can only contribute to a percolating cluster in one direction. It is natural to ask if there is a site analogue of directed percolation. This paper studies in some detail such a model, which exhibits a variety of critical phenomena, and is related to ordinary percolation in a number of limits.

In the model,<sup>(3)</sup> which is two-dimensional, all the sites and bonds exist and the bonds are directed, with both directions always being present. The randomness enters through a random rotation matrix (the angle of rotation  $\theta$  being 0,  $\pm\pi/2$ , or  $\pi$ ) being associated with each site. This rotation matrix then maps “incoming” bonds associated with the sites into “outgoing” bonds by rotating the former into the latter. (It is in this sense

---

<sup>1</sup> Departamento de Física, Universidad de Murcia, Murcia, Spain.

<sup>2</sup> Rutherford Appleton Laboratory, Chilton, Didcot, Oxon OX11 0QX, United Kingdom.

that the model constitutes a site analogue of directed bond percolation.) The resulting successions of bonds can be regarded as defining “trajectories”; indeed, the original motivation<sup>(3)</sup> was to construct a discrete model for charged particle motion in a magnetic field. The percolative aspect of the problem is whether the trajectories are extended or all are finite and localized, depending on the position in the parameter space defined by the probability distribution  $\{P(\theta)\}$ .

The trajectories are not simple random walks, as the rotation matrices are “quenched,” so that if a trajectory returns to a site, it must be rotated by the same angle as at the previous visit. (This is a difference from other models of random walks in magnetic fields.<sup>(4,5)</sup>) There is, however, a connection with more elaborate walks: when there are only sites with  $\theta = \pm\pi/2$  (“turning” sites) and equal proportion of each sign, then the trajectories are equivalent to “kinetic growth walk” on the (directed) Manhattan lattice.<sup>(6,7)</sup> The kinetic growth walk<sup>(8)</sup> is a *type* of self-avoiding walk where the weighting of each step is a local process, unlike an ordinary self-avoiding walk.

In certain limits there is also a direct connection to simple percolation. The limit of  $\theta$  being restricted to the values  $\pm\pi/2$  can be mapped into bond percolation on the dual lattice, with the probability of one type of turning sign corresponding to that of occupied bonds and the probability of the other type of sign to that of empty bonds.<sup>(3)</sup> (Thus, the case of equal probabilities coincides with the critical point for bond percolation.) This limit of only turning signs is strictly equivalent to the random tiling model of Roux *et al.*,<sup>(9)</sup> which was proven to be also equivalent to standard bond percolation.<sup>(10)</sup> The line  $P(\pi) + P(\pi/2) = 1$  [or with  $P(-\pi/2)$ ] corresponds to site percolation, with the “backwards” ( $\theta = \pi$ ) playing the role of the empty sites and the turning signs that of the occupied sites.<sup>(3)</sup> The trajectories reside on the interface between the two types of sites and can be extended at the site percolation point [ $P(\pi/2) = P_c$ ].

Indeed, the mapping onto bond percolation has been used to determine the fractal dimension of the percolation perimeter.<sup>(11)</sup> This fractal dimension ( $d_f = 7/4$ ) was conjectured by Sapoval *et al.*<sup>(12)</sup> and was subsequently derived exactly by Saleur and Duplantier.<sup>(13)</sup>

The hull of the percolation clusters (in site percolation) has been related to certain self-avoiding walks with memory by Ziff *et al.*,<sup>(14)</sup> in the square lattice, and by Weinrib and Trugman,<sup>(15)</sup> in the hexagonal lattice. The algorithms to generate these walks are equivalent to our model in the limit corresponding to site percolation. (In the case of the hexagonal lattice it again corresponds to having only backward and just one type of turning signs.) Ziff,<sup>(16)</sup> accepting the conjecture of Sapoval *et al.*, obtained other critical percolation perimeter exponents and made numerical tests of

some of them, using the previously mentioned perimeters generating algorithm.<sup>(14)</sup>

Although the model contains simple percolation, does it contain other types of critical behavior? In this paper we show that there are critical surfaces in the parameter space  $\{P(\theta)\}$  away from points that map onto ordinary percolation points. Moreover, we shall show that the critical exponents indicate that the transitions are not in the same universality class as simple percolation.

The plan of the paper is as follows: in the next section we define the model precisely and discuss some of its elementary properties; in the third section we demonstrate the existence of a critical surface in the parameter space and calculate the critical exponents; in the fourth section we use the model to determine to great accuracy the value of  $p_c$  for site percolation on a square lattice; finally, in the fifth section we discuss extensions of our work and conclude.

## 2. MODEL AND CRITICAL POINTS

In this section we define the model, discuss its elementary properties, and note the existence of critical points associated with maps onto the percolation problem. We discuss how to characterize the critical points (and their vicinities), noting the relationship between the probability distribution function of the trajectory lengths and the perimeter distribution of percolation clusters.

The model consists of an underlying lattice (square in this paper) with an “instruction” defined at each site; the trajectories are constructed by following the instructions. To be more precise: a particular realisation of the model is a lattice of sites with a two-dimensional rotation matrix  $R(\mathbf{n})$  associated with each site  $\mathbf{n}$ . The magnitude  $\theta$  of the rotations may be 0,  $\pm\pi/2$ , or  $\pi$  sites, with these values being called forward, left, right (or generically turning), and backward sites, respectively. The magnitudes are picked at random, with no correlation between different sites. A particular realization (or configuration) may be characterized by the set of probabilities  $\{P(\theta)\}$  that a randomly picked site will have magnitude  $\theta$ . This set of parameters contains the important information; a convenient way to denote the points in this parameter space is to use the “coordinate system”  $(P(0), A, P(\pi))$ , where  $A = P(\pi/2) - P(-\pi/2)$  (see Fig. 1).

A trajectory is denoted by the set  $\{\mathbf{r}(s)\}$ , where  $\mathbf{r}(s)$  is the position of the “particle” or the front of the trajectory at time step  $s$ . The rotation matrix on a site rotates incoming directions into outgoing ones. Note that this is a one-to-one relationship, so the trajectory cannot branch, merge, or end. It is also important to note that the  $R(\mathbf{n})$  do not depend on the time

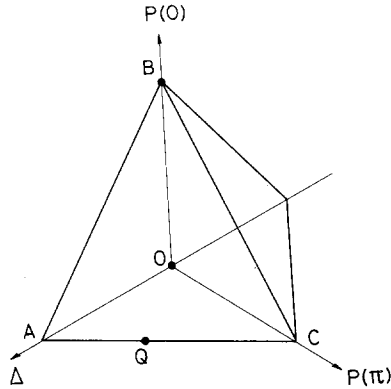


Fig. 1. The parameter space.  $B$  is the ballistic point, and  $O$  and  $Q$  are the points corresponding to bond and site percolation, respectively.

step—if the trajectory returns to a site, the same value of  $\theta$  must be used. A consequence of these two points is that all trajectories must either be infinite or cyclic, and, moreover, that any trajectory which is contained in a finite area of the lattice must be cyclic.

The most significant issue with this model is: are there regions of parameter space where the trajectories are extended? Isolated “critical” points exist, where there are extended trajectories, (trivially) at the “ballistic” point,  $(1, 0, 0)$ , and (less trivially) at  $(0, 0, 0)$  and  $(0, p_c, 1 - p_c)$ , where  $p_c \simeq 0.5928$ ; they are shown in Fig. 1. The latter two points come from mapping the model onto bond and site percolation, respectively ( $p_c$  is the critical probability for site percolation on the square lattice).<sup>3</sup>

Since we have defined the model in a dynamical manner, it is natural to describe the properties in terms of the trajectories. The simplest characterisation is the number of trajectories as a function of arc length  $s$ ,  $n(s)$  (note that this is zero for  $s$  odd). We will assume that any critical behavior is manifested by some change in this function at the critical points in the parameter space. By analogy with familiar critical phenomena, we suppose that the asymptotic behavior (at large  $s$ ) of this function is of the form

$$n(s) = s^{-\tau} f(\lambda^{1/\sigma} s) \underset{s \rightarrow \infty}{\sim} \frac{e^{-\lambda s}}{s^\tau} \quad (1)$$

Here  $f(z)$  is a scaling function, with the asymptotic form, for large  $z$ , as shown. We will comment on the form assumed for  $n(s)$  (i.e., the functional form of the argument of the exponential) in the next section.

It is plausible (assuming a “second-order” transition) that as a point with extended trajectories is approached,  $\lambda^{-1}$  will diverge, leaving a power-

law trajectory distribution  $n(s)$  at the critical point, characterized by the exponent  $\tau$ . We define the exponent for the divergence of  $\lambda^{-1}$  to be  $\sigma$ , i.e.,

$$\lambda \underset{x \rightarrow x_c}{\sim} |x - x_c|^\sigma \quad (2)$$

where  $x$  is an appropriate variable to measure the approach to the critical point at  $x_c$ . Both  $\tau$  and  $\sigma$  will be studied by Monte Carlo simulation in the following section of this paper.

The issue of the appropriate parameter  $x$  is in general a difficult point. In the case of the lines which can be mapped onto percolation problems, the choice of  $x$  is determined by the mapping (see Fig. 1): it is  $2A$  in the case of the point  $(0, 0, 0)$  and the line  $OA$  ( $x_c$  corresponds to  $A=0$ ); and  $P(\pi/2)$  in the case of  $(0, p_c, 1 - p_c)$  and the line  $AC$  [ $x_c$  there corresponds to  $P(\pi/2) = p_c$ ]. However, for other directions of approach to critical points the model does not give a natural parameter.

The existence of critical points leads naturally to the question of the existence of an order parameter. In particular, if the critical points form a surface that divides the parameter space into more than one region, is there an "expectation value" which is zero in some regions and not in others? Or perhaps a quantity that jumps between different values upon crossing a boundary between regions? We will return to this issue presently.

### 3. CRITICAL SURFACES AND EXPONENTS

In this section we report the results of numerical simulations of the model. In particular we will discuss the surface of critical points that is found in the parameter space, the exponents  $\tau$  and  $\sigma$  that we defined in Section 2, and finally the exponents associated with the moments of the function  $n(s)$ . These results allow greater precision in the determination of the corresponding quantities for the percolation perimeter. The numerical method used to determine  $n(s)$  is described in Salmerón *et al.*<sup>(17)</sup> The size of the sample was  $1400 \times 1400$  lattice sites, unless stated otherwise. The number of trajectories measured for each run was 10,000, except for the determination of the critical surface, where between 1000 and 5000 were used, and for the calculation of the exponent  $\tau$ , where up to 120,000 trajectories were simulated. The data are grouped into bins each one being 1.33 times larger than the previous one.

#### 3.1. The Critical Surface

The maps to the percolation problem yield two critical points in the parameter space; are these points connected by a "critical line" or possibly

a surface? There are two possible ways to determine the position of critical loci: count the fraction of bounded trajectories and look for the minimum along lines in the parameter space; or look for the places where  $\lambda = 0$ . In fact the former is much more accurate than the latter, since once the length scale  $\lambda^{-1}$  is greater than the system size, it is an unreliable measure of anything. However, the number of bounded trajectories retains its meaning, with the proviso that it is the number whose *spatial* extent (as against arc length) is smaller than the system size. A crucial factor in determining the accuracy of estimation of the critical surface is the proportion of forward sites: once this is of the order of half of the sites, it becomes very difficult to obtain the location (or even decide the existence) of the critical surface. Conversely, in the plane defined by  $P(0) = 0$  the transition is very sharp.

Figure 2 represents the critical surface in the region of the parameter space with  $P(0) < 0.5$ . The lines represent the intersections of the critical surface with planes of constant  $P(0)$  in steps of 0.1.

In the case of  $P(0) = 0$ , the critical line indeed connects the two critical points associated with maps to percolation. However, near  $(0, 0, 0)$  (the point  $O$  in Fig. 1) the line shows some curvature and it is difficult to estimate the angle which the line makes with the axes. Indeed, the behavior in the neighborhood of the  $P(0)$  axis is peculiar in general: the sections through the critical surface for higher values of  $P(0)$  initially move away from the  $P(0)$  axis down the  $P(\pi/2)$  axis and subsequently return to it when  $0.3 < P(0) \lesssim 0.4$ .

Further evidence of the criticality will be presented in the next subsection.

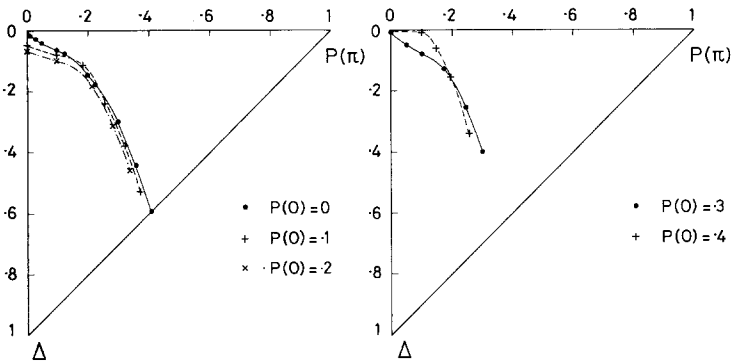


Fig. 2. The critical surface in the region  $P(0) < 0.5$ . The lines represent the intersections of the critical surface with planes of constant  $P(0)$ .

### 3.2. The Critical State: The Exponent $\tau$

The exponent  $\tau$  characterizes  $n(s)$  at the critical point and hence is a measure as to whether the different points on the critical surface are in the same "universality class." Since the points that we have discussed so far have been equivalent to percolation (excluding the "ballistic point"—see below) it is possible that the critical surface joining them has the same exponent as that implied by percolation. The case of the ballistic point,  $(1, 0, 0)$ , is a little unusual in that all trajectories are clearly infinitely long. Thus  $\tau = 0$ ; the closest analogy is a (classical) phase transition at zero temperature, where the critical state is ordered.

First we consider the two points  $O$  and  $Q$  (see Fig. 1) associated with percolation. In the case of  $O$  we find  $\tau = 2.145 \pm 0.003$ , and in the case of  $Q$  we find  $\tau = 2.146 \pm 0.003$ ; the data are shown in Figs. 3 and Fig. 4, respectively. (Due to the manner in which we generate the trajectories and the geometric progression of the bin size, the exponent is larger than that obtained directly from the figure by the additive factor of two.) In Fig. 3 (and Fig. 4) we also show the data appropriate for the percolation perimeter: in the case of  $O$ , the number of "empty" and "occupied" bonds which define the perimeter; in the case of  $Q$  we show the number of empty and occupied sites. The values of the exponent  $\tau$  obtained from the perimeters are  $2.147 \pm 0.007$  in the case of  $O$  and  $2.150 \pm 0.007$  in the case of  $Q$ . Within the errors the slopes of the number of sites in the perimeter and the number of steps in our model agree; however, the latter function yields a straight line over a greater range of  $\ln s$ . The deviations at the left-

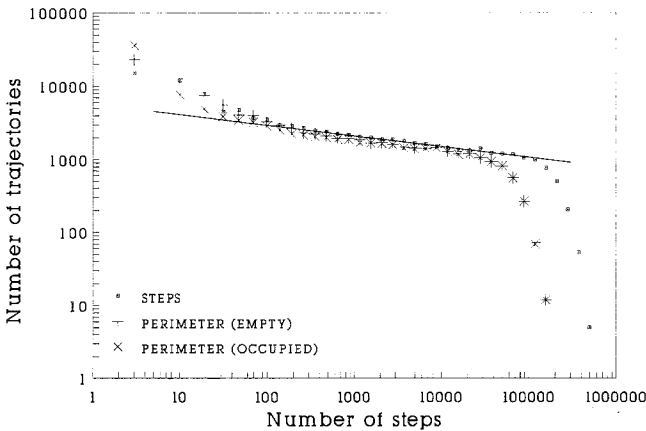


Fig. 3. Number of trajectories as a function of the number of steps and of the number of empty and occupied bond defining the perimeter for the bond percolation point  $O$ .

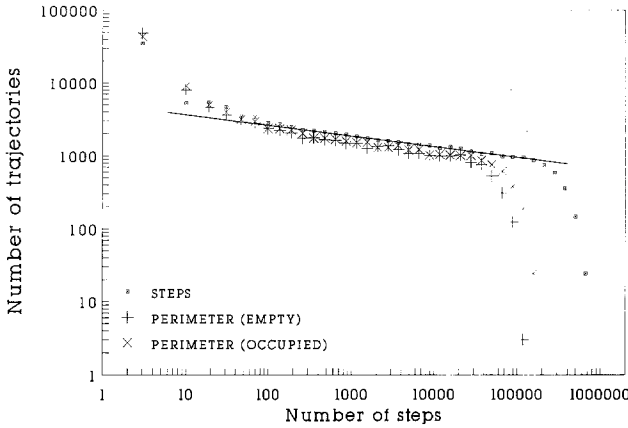


Fig. 4. Number of trajectories as a function of the number of steps and of the number of empty and occupied sites defining the perimeter for the site percolation point  $Q$ .

hand and right-hand ends of the graph are caused by the validity of the functional form assumed for  $n(s)$  (which is only valid for large  $s$ ) and finite-size effects of the sample, respectively. These values of  $\tau$  are in agreement, within errors, with Ziff's conjecture  $\tau = 15/7 \simeq 2.143$  and his numerical estimate.

We have measured the trajectory length distribution and the exponent  $\tau$  for several points on the critical surface. For all of them we found no hint of an exponential part of  $n(s)$ , indicating that they are genuine critical points. In Fig. 5 we show the value of  $\tau$  for these critical points in terms of

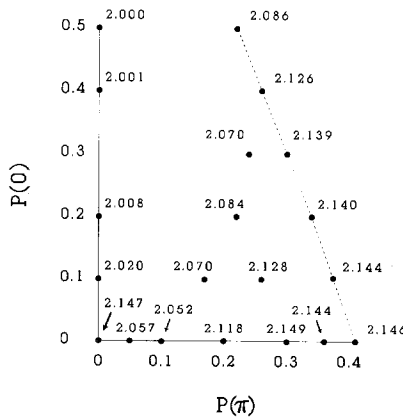


Fig. 5. Value of the exponent  $\tau$  for different points of the critical surface, in terms of their forward and backward probabilities.



their forward and backward signs probabilities (the remaining turning probabilities can be obtained from Fig. 2 and the fact that they all add up to unity). The error bars range between 0.004 and 0.008, except for the two percolation points.

The general trend for  $\tau$  is a smooth variation from the percolation values at  $O$  and  $Q$  toward 2.000 as we approach the ballistic point  $B$ . The decrease from  $O$  to  $B$  is much faster than that from  $Q$  to  $B$ . The line joining the two percolation points deserves special attention:  $\tau$  is fairly constant near  $Q$ , but it decreases sharply as we approach  $O$ .

It should be noted that the line with no backward sites in Fig. 5 does not correspond to the  $P(0)$  axis in the interval  $0 < P(0) \lesssim 0.35$ , but follows the shape shown in Fig. 2. We have been particularly careful in checking that the  $P(0)$  axis is not critical in the previous interval. In Fig. 6 we show  $n(s)$  for the point  $(0.2, 0, 0)$  and it is clear that a power law (in  $s$ ) does not fit the data. On the other hand, the point  $(0.4, 0, 0)$  demonstrates good critical behavior.

The most striking result in this section is the variation of  $\tau$  on the critical surface, implying that the points at different places on the surface may belong to distinct universality classes.

### 3.3. The Typical Trajectory: The Exponent $\sigma$

The form of the distribution function  $n(s)$  [Eq. (1)] was determined in the  $P(0)$  plane for three lines approaching the two critical points corresponding to percolation. From these results we determine, for the first time,

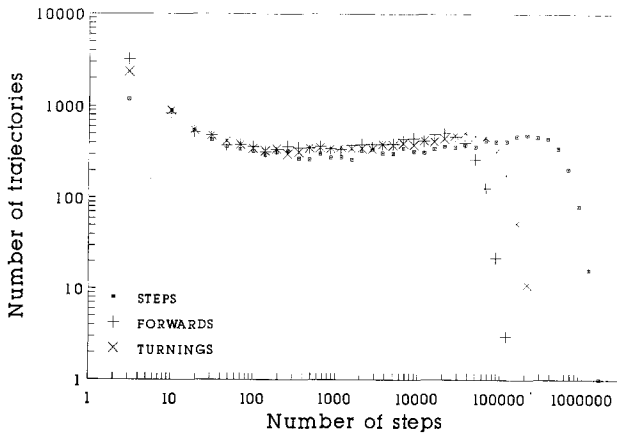


Fig. 6. Number of trajectories as a function of the number of steps and of the number of forward and turning sites visited for the point  $(0.2, 0, 0)$ .

to our knowledge, the exponent  $\sigma$  associated with the divergence of the typical perimeter length.<sup>(1)</sup>

We concentrate on the asymptotic, large- $s$ , behavior of the distribution function, as  $\sigma$  is most readily derived from there. We know the asymptotic cluster number distribution, *below*  $p_c$ , has the form of (1) (and of course it is the form of correlation functions in thermal statistical physics). However, the form of the asymptotic cluster distribution *above*  $p_c$  is quite different, with the power of  $s$  in the *exponential* being  $1 - 1/d$ , not unity. More germanely, there are scaling arguments, relating cluster size to perimeter length, which state that the perimeter distribution should not be of the form of (1). Instead it has  $s^x$  in the exponential, where Ziff's conjecture is  $x = 13/12$ .

We anticipate, since the trajectories that turn *net* left and right, for  $p < p_c$  (in the case of right and backward sites), correspond to external and internal perimeters, respectively, that the perimeter distributions will be different for these two cases. This is because one is associated with clusters of sites above  $p_c$  and the other is associated with clusters below  $p_c$ ; hence the cluster numbers (and hence perimeters) have different asymptotic forms. This was investigated by fitting the numerical data with the different functional forms ( $s$ ,  $s^x$ , and  $s^{x/2}$ ) for the argument of the exponential, the latter two corresponding to the perimeter exponents associated with the clusters below and above  $p_c$ . We find that the first two forms fit the asymptotic form of the data for the exterior perimeters equally well; however, the last does not. Conversely, the last fits the interior perimeter well, but not the exterior distribution well. For the case  $p > p_c$  the converse is true: the functional forms  $s$  and  $s^x$  for the argument of the exponential fit well the internal perimeters, while the functional form  $s^{x/2}$  is adequate for the external perimeters.

As the statistics of the internal perimeters above  $p_c$  and external perimeters below  $p_c$  are much better than the converse, we use them to determine the exponent  $\sigma$  for both the perimeters and the clusters themselves. We can calculate these exponents by fitting the two forms (the simple exponential and the exponential of  $s^x$ ) to the data. The results are shown in Fig. 7; the  $\sigma$ 's corresponding to the clusters and the perimeters, respectively, are  $0.392 \pm 0.004$  and  $0.426 \pm 0.004$  for the case of the line  $(0, x, 0)$  (bond percolation). Similar results are obtained for the line  $(0, x, 1 - x)$ , (site percolation); they are, respectively,  $0.394 \pm 0.004$  and  $0.426 \pm 0.004$ .

Ziff conjectured that  $\sigma = 3/7 \simeq 0.429$ , which agrees with our data, within errors. The exact result for the bulk exponent is  $\sigma = 36/91 \simeq 0.396$ , again in agreement with our calculation.

For those lines in the parameter space that can be mapped onto per-

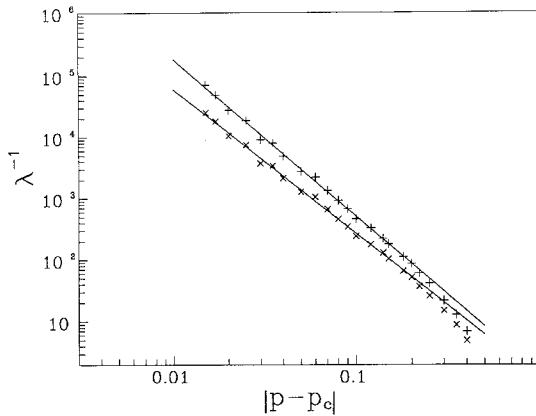


Fig. 7. Typical size  $\lambda^{-1}$ , corresponding to clusters (+) and to perimeters (x), as a function of  $|p - p_c|$  for bond percolation.

colation problems, we see that we find the expected behavior. However, along the line  $(0, 0, x)(OC)$  we find very different behavior. The assumed functional form (1) of  $n(s)$  still fits the data very well, but the exponent  $\sigma$  no longer has the value associated with percolation:  $\sigma = 0.169 \pm 0.003$  is found. Thus, the transition is more abrupt than in the percolation cases.

### 3.4. Moments of the Trajectory Length Distribution

From  $\sigma$  and  $\tau$  all the scaling exponents can be found and, in particular, those associated with the moments of the trajectory length distribution. The second moment gives us the average number of steps in a trajectory, and is related to the exponent  $\gamma$ :

$$\sum_s s^2 n(s) \underset{s \rightarrow \infty}{\sim} |p - p_c|^{-\gamma} \tag{3}$$

For percolation, Weinrib and Trugman<sup>(15)</sup> and Ziff<sup>(16)</sup> deduce  $\gamma = (3 - \tau)/\sigma = 2$ , independent of the correlation-length exponent  $\nu$ .

We have obtained the average number of steps as a function of the rotation signs probabilities along the same three lines used in the calculation of  $\sigma$ . The results for the line  $(0, x, 0)$  are shown in Fig. 8. The exponent  $\gamma$  is equal to the slope of the straight line fitting the data, and the result is  $\gamma = 2.01 \pm 0.01$ . Along the other percolation line,  $(0, x, 1 - x)$ , the result is  $\gamma = 2.002 \pm 0.006$ . The agreement with the expected value<sup>(15,16)</sup> and a previous simulation<sup>(14)</sup> ( $\gamma = 2.0 \pm 0.1$ ) is again very good. Away from

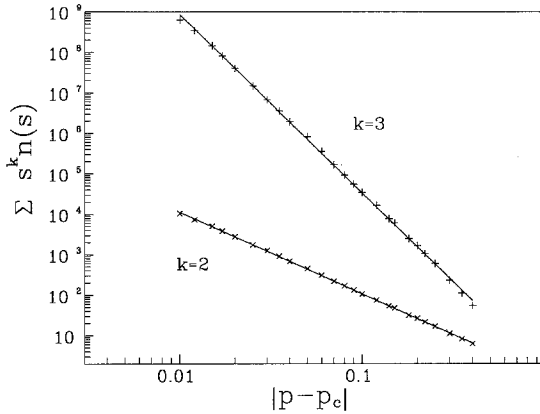


Fig. 8. Second ( $\times$ ) and third ( $+$ ) moments of the trajectory length distribution as a function of  $|x - 0.5|$  along the line  $(0, x, 0)$ .

percolation, completely different values for the exponents are obtained: along the line  $(0, 0, x)$ ,  $\gamma = 5.47 \pm 0.03$ .

We have calculated the third moment of the trajectory length distribution along the line  $(0, x, 0)$  and the results are also shown in Fig. 8. The slope of the fitted line is  $4.38 \pm 0.02$  and it should be equal to  $(4 - \tau)/\sigma$ . The difference between this and  $\gamma$  is just  $1/\sigma$ ; this constitutes a nice indirect way to obtain the exponent  $\sigma$ . By this method we obtain  $\sigma = 0.422 \pm 0.004$ , in very good agreement with our previous estimate.

#### 4. A NEW ACCURATE DETERMINATION OF $p_c$

Ziff used the perimeter of percolation clusters to estimate  $p_c$  accurately. His method had the advantage of generating the perimeter without having to populate the cluster itself, allowing the determination of  $p_c$  on a small computer. Our model includes Ziff's algorithm to generate the perimeter as a special case (with only right and backward sites); for instance, the method can be extended to other 2D lattices.

In this section we will determine  $p_c$  using a different technique, finite-size scaling. The distinction between Ziff's and our calculation is in the treatment of finite-size effects. He constructs extremely long trajectories, in effect using a very large sample (of the order of 5000 sites) by utilizing a virtual memory technique. We consider smaller samples, averaging over larger numbers of trajectories, and use finite-size scaling to extrapolate to the infinite size  $p_c$ .

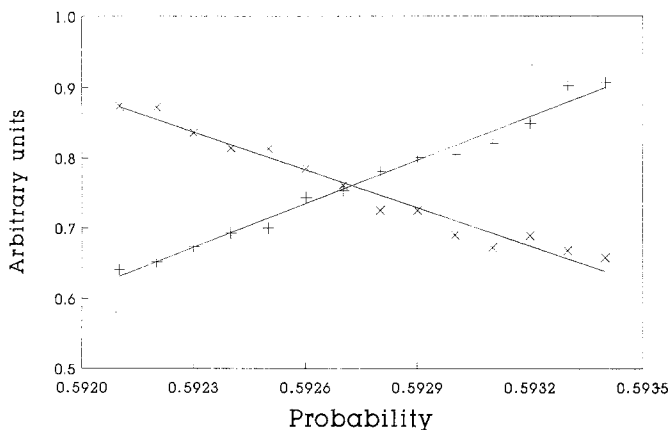


Fig. 9. Number of long trajectories,  $s > 1000$ , closing anticlockwise (x) and clockwise (+) as a function of  $x$  along the line  $(0, x, 1 - x)$  for  $L = 1000$ .

The determination of  $p_c$  for a given size of lattice  $L$  follows Ziff in that we equate the number of "external" and "internal" perimeters. In our model these correspond to trajectories turning *net* left and right, respectively. We investigated the effect of only using long—greater than 1000 steps—trajectories as against all trajectories (excluding those generated by clusters of two backward or four right sites, as they do not correspond to any perimeter).

We have performed the calculation for lattices of size 150, 250, 500, 700, 1000, and 1400, with the corresponding number of trajectories being

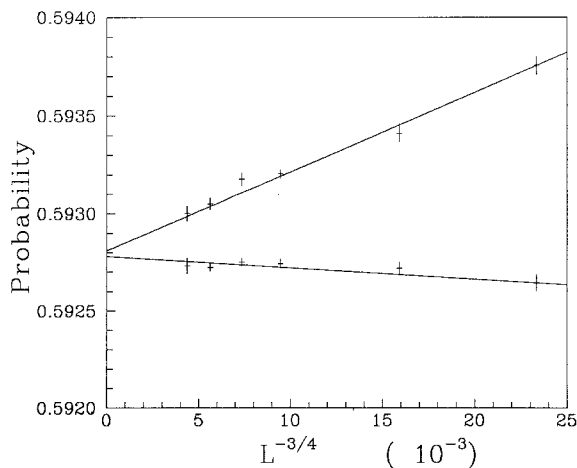


Fig. 10. Critical site percolation probabilities, corresponding to all trajectories (upper line) and only long trajectories (lower line), versus  $L^{-3/4}$ .

400,000, 200,000, 80,000, 40,000, 30,000 and 10,000. In Fig. 9 we show a typical example, for  $L = 1000$ , using only long trajectories. Ziff has noted that the principal factor in determining the high accuracy of the method is the large difference in the critical amplitudes for the average internal and external perimeter lengths.

In Fig. 10 the results for the different values of  $L$  are collected for both methods—including or excluding short trajectories. The two methods extrapolate to the same  $p_c$  within the error bars. We find  $p_c = 0.59279 \pm 0.00002$ . This is in agreement with the results of Gebele,<sup>(18)</sup>  $p_c = 0.59277 \pm 0.00005$ , of Ziff<sup>(16)</sup>  $p_c = 0.59275 \pm 0.00003$ , and in particular of Rosso *et al.*<sup>(19)</sup>  $p_c = 0.592802 \pm 0.000010$ .

## 5. CONCLUSIONS

The critical surface is perhaps the most striking result of this work. One natural question is, given that the parameter space seems to be divided into three regions, whether there is an order parameter which discriminates among these volumes. A hint as to a possible order parameter comes from the examination of the lines which can be mapped onto percolation. Along these lines there is a clear distinction between the nature of the trajectories on the different sides of the percolation points. In the case of only right- and left-turning sites, the trajectories on the left side of the transition tend to be anticlockwise and those on the right side tend to be clockwise. In the case of only backward and left (or right), the trajectories on the backward side tend to be clockwise (anticlockwise) and those on the other side tend to be the opposite. These three tendencies are not compatible, as the two backward segments, corresponding to site percolation, belong to the same region of the parameter space, but present opposite behaviors. We have tried several possible generalizations, with no success.

One of the issues that was raised in the introduction was whether the model contained critical behavior that was not in the simple percolation universality class. We have shown how the exponent  $\tau$  changes when we move away from the critical percolation points.

There are a number of generalizations of the model that could be imagined. One is to change the nature of the lattice from being square. In some ways the honeycomb lattice is simpler, as there are only three possible rotation matrices rather than four. A form of this model has been considered by Weinrib and Trugman,<sup>(15)</sup> where the rotation matrices are defined on the plaquettes, or equivalently the dual lattice. These authors were interested in constructing a model of self-avoiding walks, and hence did not consider an analogous definition on the square lattice. However, it might be interesting to ask what forms of percolation in general one could

form from variables defined on the plaquettes—a natural extension of site and bond percolation.

Finally, the extension to three dimensions is a natural generalization. We have already considered this in ref. 20. Unlike in two dimensions, no particular realization of the method can be mapped onto simple percolation. This could have been expected, since the relation between walks and percolation seems to be closely related to the duality properties of the lattice.<sup>(11)</sup>

## ACKNOWLEDGMENTS

This work has been supported in part by the Dirección General de Investigación Científica y Técnica (project number PB 86-0366). We would also like to thank the British Council for financial support during part of this work. M.O. and J.R. would like to thank the Rutherford Appleton Laboratory, and J.M.F.G. the University of Murcia and the ISI Turin, for hospitality while some of this work was performed.

## REFERENCES

1. D. Stauffer, *Introduction to Percolation Theory* (Taylor and Francis, London, 1985).
2. G. Grimmett, *Percolation* (Springer-Verlag, Berlin, 1989).
3. J. M. F. Gunn and M. Ortuño, *J. Phys. A* **18**:L1095 (1985).
4. B. Y. Bologurov, *Sov. Phys. Solid State* **28**:1694 (1986).
5. S. N. Dorogostev, *Sov. Phys. Solid State* **28**:1699 (1986).
6. S. S. Manna and A. J. Guttmann, *J. Phys. A* **22**:3113 (1989).
7. R. M. Bradley, *Phys. Rev. A* **41**:914 (1990).
8. I. Majid, N. Jan, A. Coniglio, and H. E. Stanley, *Phys. Rev. Lett.* **52**:1257 (1984); S. Hemmer and P. C. Hemmer, *J. Chem. Phys.* **81**:584 (1984); J. W. Lyklema and K. Kremer, *J. Phys. A* **17**:L691 (1984).
9. S. Roux, E. Guyon, and D. Sornette, *J. Phys. A* **21**:L475 (1988).
10. B. Duplantier, *J. Phys. A* **21**:3969 (1988).
11. P. Grassberger, *J. Phys. A* **19**:2675 (1986).
12. B. Sapoval, M. Rosso, and J. F. Gouyet, *J. Phys. (Paris)* **46**:1149 (1985).
13. H. Saleur and B. Duplantier, *Phys. Rev. Lett.* **58**:2325 (1987).
14. R. M. Ziff, P. T. Cummings, and G. Stell, *J. Phys. A* **17**:3009 (1984).
15. A. Weinrib and S. A. Trugman, *Phys. Rev. B* **31**:2993 (1985).
16. R. M. Ziff, *Phys. Rev. Lett.* **56**:545 (1986).
17. J. Salmerón, M. Ortuño, and J. M. F. Gunn, *Z. Phys. B* **70**:269 (1988).
18. T. Gebele, *J. Phys. A* **17**:L51 (1984).
19. M. Rosso, J. F. Gouyet, and B. Sapoval, *Phys. Rev. B* **32**:6053 (1985).
20. M. Ortuño, J. F. M. Gunn, and R. Chicón, *J. Phys. A* **20**:4047 (1987).